Virologica Sinica 38 (2023) 119–127

Contents lists available at ScienceDirect

Virologica Sinica

journal homepage: www.keaipublishing.com/en/journals/virologica-sinica
www.virosin.org

Research Article

Taurolidine improved protection against highly pathogenetic avian influenza H5N1 virus lethal-infection in mouse model by regulating the NF-κB signaling pathway

Chaoxiang Lv [a,b,1], Yuanguo Li [b,c,1], Tiecheng Wang [b,1], Qiqi Zhang [a], Jing Qi [a,b], Mingwei Sima [b,d], Entao Li [b], Tian Qin [a,b], Zhuangzhuang Shi [b,e], Fangxu Li [b,f], Xuefeng Wang [b], Weiyang Sun [b], Na Feng [b], Songtao Yang [b], Xianzhu Xia [b], Ningyi Jin [a,b,d,e,*], Yifa Zhou [a,*], Yuwei Gao [b,d,e,f,*]

[a] College of Life Sciences, Northeast Normal University, Changchun, Jilin, 130021, China
[b] Changchun Veterinary Research Institute, Chinese Academy of Agricultural Sciences. Changchun, 130122, China
[c] College of Animal Medicine, Jilin University, Changchun, 130000, China
[d] College of Basic Medicine, Changchun University of Chinese Medicine, Changchun, 130117, China
[e] College of Animal Science and Technology, Jilin Agricultural University, Changchun, 130033, China
[f] College of Life Sciences, Shandong Normal University, Jinan, 250014, China

ARTICLE INFO

Keywords:
Influenza viruses
H5N1
Taurolidine (TRD)
Cytokine storms
Inflammatory response
NF-κB signaling pathway

ABSTRACT

Taurolidine (TRD), a derivative of taurine, has anti-bacterial and anti-tumor effects by chemically reacting with cell-walls, endotoxins and exotoxins to inhibit the adhesion of microorganisms. However, its application in antiviral therapy is seldom reported. Here, we reported that TRD significantly inhibited the replication of influenza virus H5N1 in MDCK cells with the half-maximal inhibitory concentration (EC_{50}) of 34.45 μg/mL. Furthermore, the drug inhibited the amplification of the cytokine storm effect and improved the survival rate of mice lethal challenged with H5N1 (protection rate was 86%). Moreover, TRD attenuated virus-induced lung damage and reduced virus titers in mice lungs. Administration of TRD reduced the number of neutrophils and increased the number of lymphocytes in the blood of H5N1 virus-infected mice. Importantly, the drug regulated the NF-κB signaling pathway by inhibiting the separation of NF-κB and IκBa, thereby reducing the expression of inflammatory factors. In conclusion, our findings suggested that TRD could act as a potential anti-influenza drug candidate in further clinical studies.

1. Introduction

Influenza virus is the main pathogen that caused influenza. The individual infected with influenza virus could bring about acute respiratory diseases, which leads to severe pneumonia, and eventually death (Taubenberger and Kash, 2010; Viboud et al., 2016; Kain and Fowler., 2019). The virus is highly contagious and can easily cause global outbreaks. In recent years, the continuous spread of highly pathogenic avian influenza virus (HPAIV), such as H5N1, H5N8, H7N9, has seriously threatened public health (Sutton et al., 2018). With a high mutation and replication rate, HPAIV is able to quickly adapt to environmental changes and has brought great challenges to the prevention and treatment of influenza virus (Pleschka et al., 2013). The large outbreaks of avian influenza A (H5N1) often lead to human influenza A (H5N1) outbreaks. The expanding geographic distribution of avian influenza A (H5N1) infections, with recent frequent outbreaks in Asia, Europe and the Americas (Lee and Tang, 2015; Tian et al., 2015; Lewis et al., 2021), suggests that an increasing number of people are at risk. Currently, the clinical prevention strategies against influenza virus were mainly based on vaccination and antiviral treatment. However, vaccines do not fully protect against outbreaks caused by antigenically divergent strains (Mehrbod et al., 2018). The currently licensed antivirals mainly include alkylamine and neuraminidase inhibitors. The former is only effective against influenza A virus, while the latter has side effects, such as hallucinations,

* Corresponding authors.
E-mail addresses: ningyik@126.com (N. Jin), zhouyf383@nenu.edu.cn (Y. Zhou), gaoyuwei@gmail.com (Y. Gao).
[1] Chaoxiang Lv, Yuanguo Li and Tiecheng Wang contributed equally to this work.

https://doi.org/10.1016/j.virs.2022.11.010
Received 8 July 2021; Accepted 21 November 2022
Available online 28 November 2022

abnormal behavior, hearing, and vision impairment (Jacobi et al., 2005). Thus, it is very important to search for new antiviral drugs with high efficiency and low toxicity.

Taurolidine (TRD), a derivative of taurine, has important roles in the clinical treatment of anti-tumor, anti-bacterial, and anti-adhesion (Arweiler et al., 2012; Haro et al., 2019). The derivative could chemically react with cell walls, endotoxins and exotoxins, thereby inhibiting the adhesion of microorganisms and exerting anti-bacterial effects (Doddakula et al., 2010). In the peritoneum, it prevents the local recurrence and metastasis to distant organs of tumor cells by restricting the release of cytokines from macrophages (Braumann et al., 2009). Additionally, TRD inhibits the synthesis of interleukin-1 (IL-1) and tumor necrosis factor (TNF) in mononuclear cells from human peripheral blood (Bedrosian et al., 1991). TRD induces apoptosis by activating mitochondrial cytochrome-*c*-dependent mechanisms and an external direct pathway in tumor cells (Neary et al., 2014). Previous studies on taurolidine mainly focused on anti-bacterial and anti-tumor aspects, but its application in antiviral activity is rarely reported.

In this study, we evaluated the inhibitory activity of TRD on H5N1 *in vitro* and *in vivo*. Using transcriptomic and molecular biochemical approaches, we identified the important roles of TRD in reducing cytokine storm and inflammation response, as well as sought to determine their potential antiviral targets. These findings demonstrate the potential utility of TRD as an alternative antiviral agent to treat the influenza virus infection. This not only provided core technical support for the prevention and control of influenza virus, but also laid new ideas for the elucidation of the targets and antiviral mechanisms of new drugs.

2. Materials and methods

2.1. Cells culture and reagents

Influenza H5N1 virus was separated and obtained from the dead cubs in the Hengdaohezi Reserve of Heilongjiang, on August 14, 2016 (A/Tiger/Heilongjiang/HDHZ-01/2016; the GenBank accession OP782321–782328). The virus was stored in the Institute of Changchun Veterinary Research, Chinese Academy of Agricultural Sciences (Changchun, China). The study was approved by Military Medical Research Institute, and virus-related experiments were carried out in Biosafety Level-3 Laboratory (BSL-3). Six-to eight-week-old BALB/c female mice were purchased from Charles River Laboratory Animal Technology Co., Ltd (Beijing, China).

The Madin-Darby canine kidney cell line (MDCK) and the human type-II alveolar epithelial cell line (A549) were cultured in Dulbecco's Modified Eagle's Medium (DMEM) supplemented with 10% fetal bovine serum (FBS, Gibco Lot. No.10438026) with 100 μg/mL penicillin and 100 μg/mL streptomycin. Cell lines were cultured in humidified air at 37 °C with 5% CO_2.

TRD and mouse monoclonal antibody for β-actin (Cat. No. A5316) were from Sigma-Aldrich (St. Louis, MO). TRD was solubilized in PBS at 4 mg/mL. Mouse monoclonal antibody against viral nucleoprotein (NP; Cat. No. ab128193) was generously provided by Abcam Company (Burlingame, CA, USA). Rabbit polyclonal antibody against IκBa (Cat. No. #9242), *p*-IκBa (Cat. No. #2859), NF-κB (Cat. No. #8242), p–NF–κB (Cat. No. #3033), IL-6 (Cat. No. #12912) and TNF-α (Cat. No. #11948) were provided by Cell Signaling Technology (Beverly, MA, USA).

2.2. Drug treatment and inhibitory efficacy

To determine the *in vitro* antiviral effect of TRD, different concentrations of TRD (0, 5, 10, 25, 50, 100 and 200 μg/mL) were added to MDCK cells. Briefly, the cells were infected with influenza virus H5N1 at a multiplicity of infection (MOI) of 0.1 for 12 h, and then cultured for 48 h with different concentrations of TRD. To determine the active stage of TRD against influenza virus H5N1, we treated MDCK cells with three different infection protocols, including pre-treatment, co-treatment and post-treatment. (1) Pre-treatment: the cells were treated with TRD (50 μg/mL) for 2 h before virus infection, and then the virus was inoculated into cells after discarding the cell culture supernatant. (2) Co-treatment: the virus was incubated with TRD (50 μg/mL) for 15 min and then inoculated into cells. (3) Post-treatment: TRD (50 μg/mL) was added to cells after virus inoculation for 12 h.

Then, the cytopathic effect (CPE) was observed with electron microscopy, and the cell viability was measured by MTT assay. The effective inhibition rate of the TRD was calculated using the following equation: inhibition rate (%) = (mean optical density of TRD - mean optical density of virus controls)/(mean optical density of cell controls - mean optical density of virus controls) × 100. The concentration for 50% of maximal effect (EC_{50}) was calculated using fitted curves.

2.3. Virus titration

Titers of influenza virus in the supernatants of treated cells or lung tissues were quantified by estimating the 50% tissue culture infectivity doses ($TCID_{50}$). MDCK cells were seeded at a concentration of 1×10^4 cells/well into 96-well tissue culture plates, and on the next day, the tenfold diluted supernatants were added and cultured for 48h. Before calculating $TCID_{50}$ by CPE observation, cell viability was determined by MTT assay. Finally, the Reed-Muench method was used to calculate the virus titration, the result expressed as $\log_{10}TCID_{50}$. For viral RNA copy number detection, the total intracellular RNA was extracted after virus infection, and the viral *M* gene was amplified by RT-qPCR, the primer sequences listed in Supplementary Table S1.

2.4. Cytotoxicity assay

The MDCK cells were adjusted to 1×10^5 cells/mL, and inoculated into 96-well plate (100 μL/well). Varies concentrations of TRD (ranging from 0 to 800 μg/mL) were added to cell culture. After incubation for 48 h, the cell morphology was observed and photographed using an electron microscope (JEM 1011; JEOL). Then, 10 μL MTT was added to each well (5 mg/mL, Sigma Chemicals Co.) and incubated for 4 h. Next, 200 μL DMSO was added to each well and incubated at 37 °C for 10 min in dark. Subsequently, the absorbance values (OD) at 570 nm were measured and recorded.

2.5. Hemagglutination test (HA)

The MDCK cells infected with influenza virus H5N1 were divided into three groups, DMSO-treated group (5 μg/mL, 50 μg/mL), TRD-treated group (5 μg/mL, 50 μg/mL) and oseltamivir (OSTA)-treated group (5 μg/mL, 50 μg/mL). After the cells were treated for 48 h, 50 μL of the cell supernatant was added to a 96-well microhemagglutination plate. Then, using 1% washed chicken red blood cells (RBC) as the indicator system, 50 μL of RBC suspension was added to each well. Before observing the results, the samples were left to stand at room temperature (15–30 °C) for 15 min.

2.6. Immunofluorescence and immunohistochemistry assay (IFA and IHC)

Samples were harvested and washed three times with PBS, and then fixed in 4% paraformaldehyde for 45 min at room temperature (15–30 °C). After that, primary antibodies were added and incubated overnight at 4 °C. Then, the samples were washed three times with PBS and incubated second antibodies for 2–3 h at room temperature (15–30 °C). Then, samples were stained with Hoechst (CST, CAS, NO: 23491-45-4) for 20 min. For immunohistochemistry, samples were infiltrated and paraffin-embedded to prepare ultrathin sections (3–5 μm thick) before deparaffinization with xylene and alcohol baths. The sections were soaked in antigen retrieval solution for 10 min to block endogenous peroxidase after soaking in 2% H_2O_2 for 5–10 min. Subsequently, PBS containing 5% bovine serum albumin was added to the sections for blocking to block

nonspecific sites. Before binding to the corresponding secondary antibodies, the primary antibodies against p–NF–kB (1:200) were added and incubated overnight at 4 °C. Then, images (200 × and 400 × magnifications) were observed and photographed using a resolving microscope (JEM 1011; JEOL). The positive area densities and positive cell ratios were analyzed using the Image-Pro Plus 6.0 system (Media Cybernetics Corporation, USA). Positive cell ratios = number of positive cells/total number of cells.

2.7. Mice infection and cytokine transcriptome analysis

The mice (16–22 g) were divided into a control group (control, uninfected), a virus group (virus, infected), and taurolidine intramuscular injection group (Virus + TRD, post-infection TRD treatment), with 7 mice in each group. Mice were inoculated intranasally (i.n.) with 20 × LD_{50} (50% mice lethal dose) mouse-adapted A/Tiger/Heilongjiang/HDHZ-01/2016 (H5N1) virus suspended in 50 μL normal saline. After infection for 6 h, TRD (200 mg/kg) was given to the treatment twice daily (morning and evening, total 400 mg/kg/d) for 5 days by intramuscular injection. The body weight of each group of mice was measured every day, and the survival status of each mouse was also observed. The body weight and survival were observed daily for two weeks. The mice were randomly selected for euthanasia for lung pathological examination in each group (n = 3) on day 3 and day 5 after infection. Lung index was defined as the percentage of lung weight to body weight (Lung index = lung weight/body weight × 100). For cytokine transcriptome analysis, we examined lung-wide gene expression (transcriptomic) in each group of mouse models and selected GSEA (version 4.0.3) to determine phenotypic differences. The cytokine transcriptome heatmaps were visualized by the R pheatmap package (version 4.0.1).

2.8. Immunoblotting and co-immunoprecipitation analysis

For Western blotting, isolated cells or tissues protein lysates were separated by 10% SDS-PAGE and blotted onto PVDF, which were then incubated with specific antibodies after blocking with 5% bovine serum albumin (BSA, Sigma, CAS, NO: 9048-46-8) in Tris-buffered saline with Tween 20 (TBST). Then, the PVDF membranes were incubated with the secondary antibody for 1 h at room temperature (15–30 °C). An Easysee Western Blot Kit (Transgene, Alsace, France) was used to blot samples.

For co-immunoprecipitation, we used to assess NF-κB and IκBa complex formation. A549 cells were treated with or without 50 μg/mL TRD at 12 h post-infection. After 24 h, cell lysates were collected from each group, including the uninfected group, the infected group, and the TRD-treated infected group. Then, each group of cell lysates were cross-linked with dithio-bis succinimidyl propionate for 30 min. Subsequently, pre-cleared lysates were then incubated with pre-equilibrated protein-A or protein-G-Sepharose beads with either NF-κB or IκBa antibody overnight at 4 °C. The eluted-protein was analyzed by immunoblotting using NF-kB (1:1000) and IkBa (1:1000) antibodies.

2.9. Quantitative real-timePCR (qRT-PCR)

Quantitative analysis of *M*, *IL-6*, *CCL2*, *CXCL2*, *IFNγ*, *CXCL3*, *TNF-α*, *IL2*, *IL-1β*, *CCL5*, *IFNα* and *Actin* (loading control) mRNA levels was performed by qRT-PCR method using a 2 × Power SYBR Premix Ex TaqTM (TaKaRa Bio INC, Japan) in a Bio-Rad iCycler & iQ qRT-PCR systems (Bio-Rad, Hercules, CA, USA). The sequences of the forward and reverse primers were listed in Supplementary Table S1.

2.10. Pulmonary pathology assay

Mice were randomly selected from the control group, virus group, and therapeutic group and euthanatized. Lung tissues were quickly removed and placed in 4% paraformaldehyde (PFA) for 24–72 h. Tissue samples were embedded in paraffin and randomly cut into 5–10 μm slices. Subsequently, the sections were stained with hematoxylin-eosin (HE) for 3–5 min and observed under an optical microscope. The pathology scores are summarized according to hemorrhage, alveolar wall thickening, inflammation and cell necrosis.

2.11. Hematological analysis

The whole blood was collected in EDTA-anticoagulation tubes, and an automatic hematology analyzer (Mindray Medical, BC-5000, China) was used for hematological analysis. The hematological parameters included the average total white blood cell counts (WBC), lymphocyte counts (Lymph), and neutrophil counts (Gran), monocytes counts (Mon) and platelets counts (PLT). Lymph (%) = (mean Lymph counts)/(mean WBC counts) × 100. Gran (%) = (mean Gran counts)/(mean WBC counts) × 100. Mon (%) = (mean Mon counts)/(mean WBC counts) × 100.

2.12. Enzyme-linked immunosorbent assay (ELISA)

Serum samples from different groups of mice were collected. The concentration of TNF-α, IL-1β and IL-6 in the serum were determined by ELISA according to the instructions of the manufacturer (Jing Mei Co., Ltd., China).

2.13. Statistical analysis

Statistical comparisons were performed using ANOVA analysis. Quantitative data sets were expressed as the means ± standard error (SE), and the statistical significance was evaluated by Graphpad Prism 8.0 software. Relative to the control, $*P < 0.05$, $**P < 0.01$ and ***, $P < 0.001$ versus the control were regarded as significant.

3. Results

3.1. TRD inhibited the propagation of influenza virus H5N1 in vitro

To evaluate the potential anti-viral effect of anti-bacterial TRD, the toxicity inhibition assay in MDCK cells was examined. TRD showed significant anti-virus activity and inhibited the reproduction of the virus with the half-maximal effect concentration (EC_{50}) of 34.45 μg/mL (Fig. 1A). The cytotoxicity of TRD on MDCK was evaluated using MTT assay, and the half-maximal cytotoxicity concentration (CC_{50}) of 231.5 μg/mL (Fig. 1B). In order to clarify the active stage of TRD against influenza virus H5N1, we treated MDCK cells with three different infection protocols, including pre-treatment, co-treatment and post-treatment. We found that post-treatment TRD exhibited high inhibition rates in H5N1-infected MDCK cells (Fig. 1C), which indicating that TRD had a significant inhibitory effect on the replication and release of influenza virus H5N1. Cell morphology after TRD treatment at a concentration of 50 μg/mL were also investigated, and no cellular changes was observed in MDCK and A549 cells (Fig. 1D). Those results indicated that TRD can inhibit H5N1 replication and has no cytotoxicity on MDCK and A549 cells. Thus, we chose the low toxic dose (50 μg/mL) for following studies.

To further explore the potential antiviral effects of TRD, we performed a virus titration assay in MDCK cells and selected oseltamivir (OSTA) as a positive control. TRD and OSTA treatment cell groups showed significantly lower virus titer than the DMSO-treated group (Fig. 1E). This inhibitory effect of TRD was confirmed in the hemagglutination inhibition test (Fig. 1F). Subsequently, the inhibitory effects of TRD and OSTA were further assessed by IFA in A549 cells. The nuclear appearance of the viral nucleoprotein (NP) was quantified as the output of successfully infected cells (Fig. 1G). Compared with DMSO-treated control cells, the ratio of NP-positive cells was significantly reduced by 16.78% after TRD treatment (Fig. 1H). We further confirmed the inhibition of TRD in A549 cells by Western blot assay. The result showed that drug treatment significantly reduced the expression of viral NP protein in

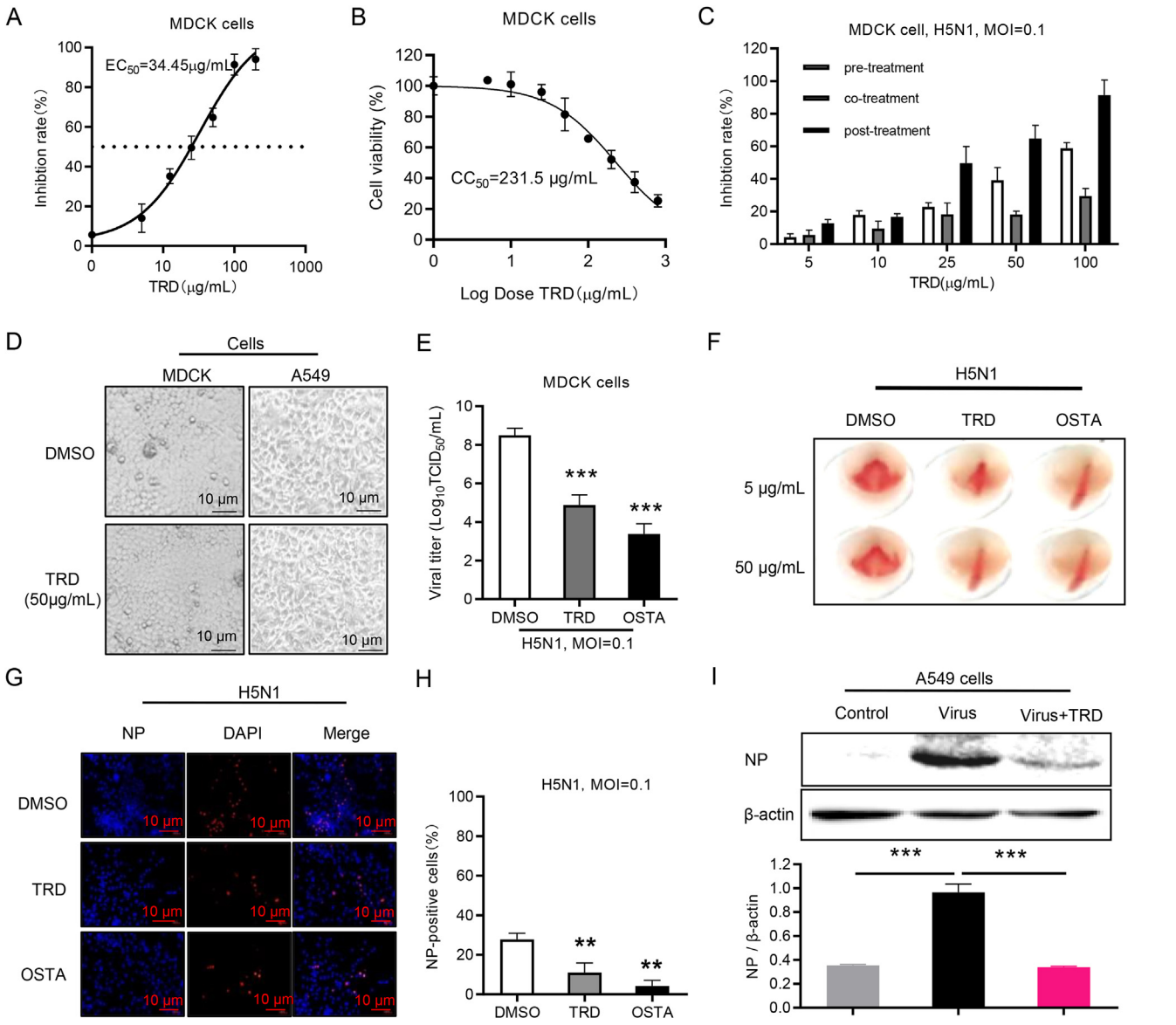

Fig. 1. Inhibitory effects of TRD on influenza viruses H5N1 *in vitro*. **A** Inhibition rate of TRD (0, 5, 10, 25, 50, 100 and 200 μg/mL) against influenza virus H5N1 (MOI = 0.1) in MDCK cells. The EC_{50} value was calculated by semi-logarithmic fitting curve. **B** Cellular toxicity of TRD in MDCK cells was evaluated by MTT assay. **C** Inhibitory rates of TRD against influenza viruses H5N1 with different infection protocols were evaluated in MDCK cells. **D** The microscopic images of TRD-treated (50 μg/mL) MDCK and A549 cells at 48 h post H5N1-infection. **E** After infecting with H5N1 at the MOI of 0.1, MDCK cells were treated with DMSO and TRD (50 μg/mL) for 24 h, and oseltamivir (OSTA, 50 μg/mL) was used as a positive control, and virus titer was determined by virus titration assay. **F** The cell culture was collected and used to test positive virus in supernatant by hemagglutination inhibition method. **G** After A549 cells infection with H5N1 at the MOI = 0.1, the cells were treated with solvents DMSO and TRD (50 μg/mL) for 24 h, and OSTA (50 μg/mL) was used as a positive control. The nucleus was stained with DAPI, and the infected cells were detected by nuclear NP staining (scale bar 10 μm). **H** The percentage of NP-positive cells in Fig. 1G was calculated. **I** After A549 cells infected with H5N1 at the MOI = 0.1, the cells were treated with DMSO and TRD for 24 h, and the expression level of influenza NP protein in A549 cells was analyzed by Western blot assay, using β-actin as a control.

cells (Fig. 1I). These results suggested that TRD had an excellent antiviral effect against influenza virus *in vitro*.

3.2. The effect of TRD on the prognosis of H5N1 lethal challenge mice

We previously suggested that TRD showed a positive anti-viral effect *in vitro*. To better evaluate its therapeutic effect, a mouse model infected with H5N1 was used to evaluate the inhibitory effect of TRD on influenza A virus. Compared with the virus group (treated with normal saline), TRD treatment (400 mg/kg/d) protected the mice from body weight loss ($P < 0.001$; Fig. 2A). In the TRD treatment group, we observed that one mouse lost less than 25% of its body weight, but did not die. In addition, TRD treatment significantly increased the overall survival rate of animals (protection rate was 86%; Fig. 2B). Subsequently, we analyzed the viral loads in the lung tissues of mice at 3 and 5 day post-infection, and found that viral loads were significantly reduced in TRD-treat group (Fig. 2C). In addition, qRT-PCR analysis also showed that the expression of *M* gene in mouse lungs was significantly down-regulated (Fig. 2D). Western blot results also confirmed that TRD significantly reduced the replication of the virus in the lung tissues (Fig. 2E). We also found TRD treatment significantly improved the lung index (Fig. 2F).

To determine whether TRD improves the lung pathology caused by H5N1 infection, we collected the lung tissues of each group of mice to perform HE assays on the fifth day. The results showed that the virus infection caused a small number of necrotic cell fragments (red arrow), and inflammatory cells infiltrated into a ring in the bronchial lumen to

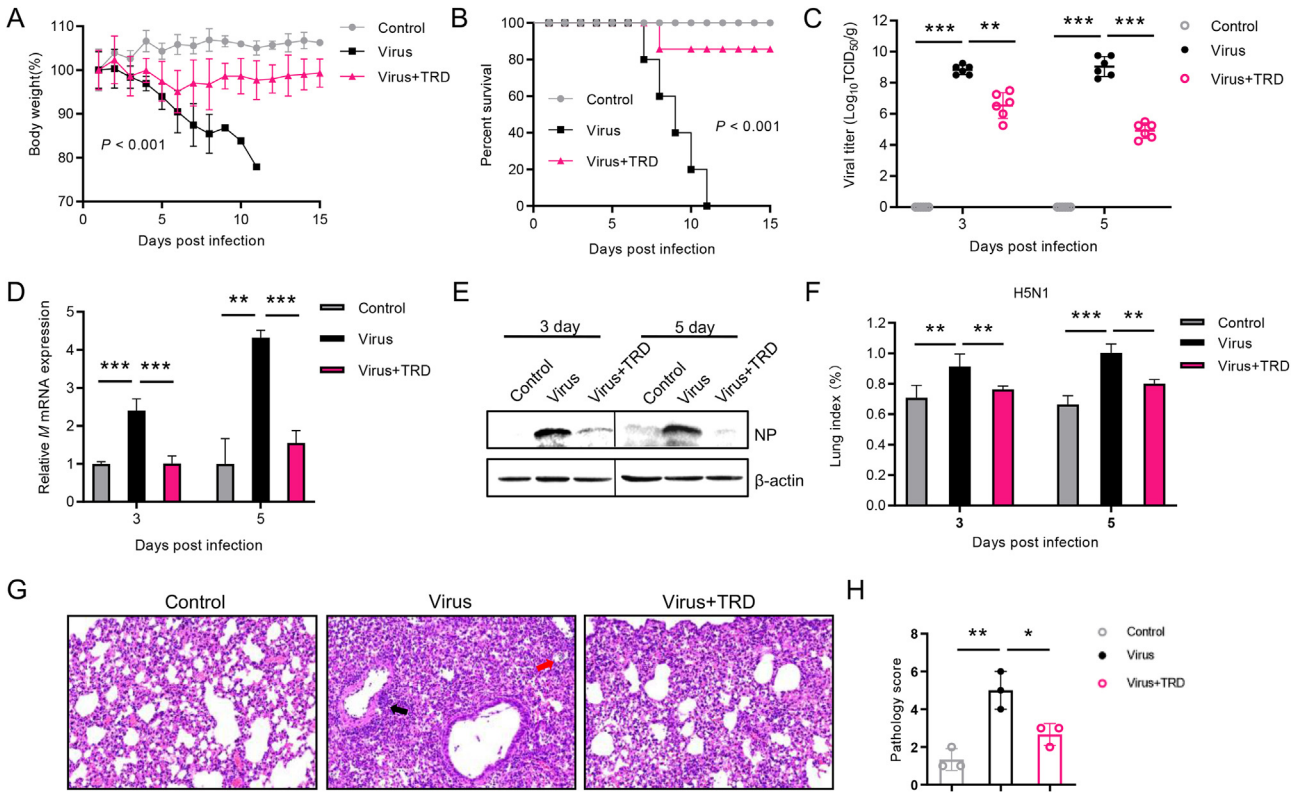

Fig. 2. The antiviral effect of TRD against H5N1 in mice model. **A** Body weight changes in control group (control, gray), virus group (virus, black) and TRD treatment group (Virus + TRD, purple). **B** Survival rate of H5N1-infected mice treated or untreated with TRD. **C** Virus titer in mouse lung tissues at the 3 and 5 day post infection (dpi) after H5N1 infection. **D** The mRNA expression levels of influenza *M* gene in mouse lung tissue were determined at the 3 and 5 dpi by qRT-PCR. *β-Actin* was used as an internal control. **E** The expression level of influenza NP protein in lung tissues of mice at 3 and 5 dpi was analyzed by Western blot, and used β-actin as a control. **F** The effect of the drug on the lung index of mice was measured on the 3 and 5 dpi after virus infection. **G** Hematoxylin-eosin staining of lung tissues of TRD treated or untreated mice. The representative images were showed here. **H** Lung pathology score on 5-dpi. The pathology scores are summarized according to (one point each for hemorrhage, alveolar wall thickening, inflammation, and cell necrosis), n = 3.

form a vascular cuff (black arrow); however, this scene was improved by TRD treatment (Fig. 2G). Histopathological scoring suggested that TRD-treated effectively attenuated the pathological damage caused by H5N1 infection (Fig. 2H). And no obvious tissue lesions presented, in heart, liver, spleen, lung and kidney after TRD administration with the dose of 400 mg/kg/d (Supplementary Fig. S1). These findings indicated that the drug treatment within a safe concentration effectively improved the pathological damage caused by H5N1 infection.

3.3. TRD inactivated the cytokine storm effect in mice

Influenza virus infection caused abnormal expression of inflammatory cytokines (Betakova et al., 2017). To investigate the effect of TRD on the inflammatory response induced by H5N1 infection, the expression of inflammatory-related genes in mouse lung tissues was studied by transcriptome analysis (Fig. 3A). Gene enrichment analysis showed that the NF-kB signaling pathway was significantly enriched (Supplementary Fig. S2A). In addition, we also found that cytokine and chemokine signaling pathways were also significantly enriched (Supplementary Figs. S2B and 2C). Differentially expressed genes (DEGs) were verified by quantitative reverse transcription PCR (qRT-PCR). We observed that TRD significantly inhibited the mRNA expression of cytokines and chemokines, including *IL-6*, *CCL2*, *CXCL2*, *IFN-γ* and *CXCL3* (Fig. 3B), as well as *TNF-α*, *IL2*, *IL-1β*, *CCL5* and *IFNα* (Fig. 3C).

As key transcriptional regulators of type I interferon (IFN)-dependent immune responses, IRF3 and IRF7 play important roles in innate immune responses against viruses (Xue et al., 2018). Thus, we examined the detection of IRF3 and IRF7 expression. The results showed that the mRNA expressions of *IRF3* and *IRF7* were up-regulated after influenza virus H5N1 infection, while their expressions were inhibited by TRD treatment (Fig. 3D and E). This inhibitory effect of TRD was confirmed in the Western blot assay (Fig. 3F). These findings indicated that the administration of TRD could blunt the cytokine storm activated by influenza virus.

3.4. The effect of TRD on NF-κB signaling pathway

The location of NF-κB in the cell determines its activity in regulating biological functions. To better understand the specific effect of TRD on NF-κB signaling pathway, immunofluorescence experiments were carried out in A549 cells. We found that the virus infection caused the transfer of NF-κB from the cytoplasm to the nucleus, and this phenomenon was reversed by the administration of TRD (Fig. 4A). NF-κB and IκBa usually exist in the form of a complex, and the activation of NF-κB depended on the phosphorylation of IκBa, which was regulated by IKK phosphorylation (Lawrence 2009). Interestingly, TRD rescued the separation of the complex caused by H5N1 infection (Fig. 4B). Western blot results showed that the virus infection reduced the expression of IκBa, promoted the phosphorylation of IκBa and NF-κB, and induced the expression of IL-6 and TNF-α (Fig. 4C). However, the administration of TRD significantly reversed the above process (Fig. 4D and E). These results suggested that TRD was able to inhibit the nucleus metastasis of NF-κB, therefore reducing the activation of inflammatory cytokines caused by H5N1 infection.

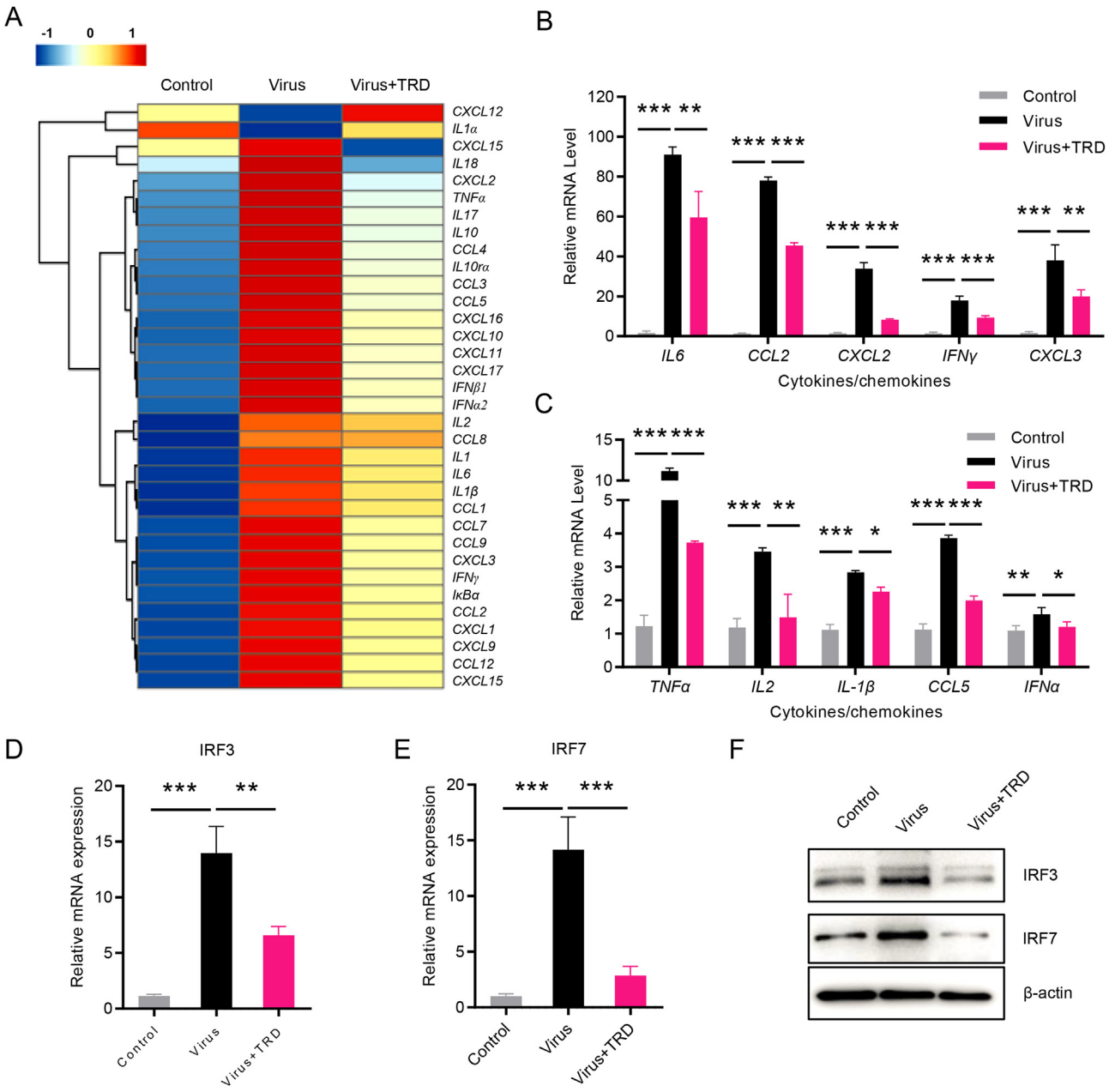

Fig. 3. The treatment of TRD blunted cytokine storm. **A** Transcriptome analysis was performed on the lung tissue from mice in control group, virus infection group, and post-infection TRD treated group on day 5, and the genes related to inflammation were analyzed by heat map. **B, C** The mRNA expression levels of pro-inflammatory cytokines and chemokines in mouse lung tissue were detected by qRT-PCR, and *β-actin* was used as an internal control. **D-E** The mRNA expression levels of *IRF3* (**D**) and *IRF7* (**E**) in mouse lung tissue were detected by qRT-PCR, and *β-actin* was used as an internal control. **F** The expression level of IRF3 and IRF7 in mouse lung tissue were detected by Western blot assay, using β-actin as a control.

3.5. TRD reduce the inflammation in mice

Nuclear expression levels of NF-κB were associated with a poor prognosis of influenza virus infection (Mulero et al., 2019). To verify suppressive effects of TRD on the inflammation *in vivo*, we used immunohistochemical method to analyze the activity of NF-κB in lung tissues with- or without-drug treatment. Our results showed that drug treatment significantly inhibited p–NF–κB expression in lung tissues at day 5 post infection (Fig. 5A), and the percentage of p–NF–κB positive cells (Fig. 5B). Interestingly, we found the increase of lymphocytes counts (Lymph) and monocyte counts (Mon) in serum by hematological analysis, as well as the decrease of neutrophils counts (Gran) at 3 dpi (Fig. 5C) and 5 dpi (Fig. 5D) after treatment with TRD. Moreover, the number of platelets and inflammatory factors in the serum were significantly reduced (Fig. 5E and F). These findings demonstrated that TRD treatment significantly improved the immunity of infected mice during pathogenic influenza virus infection.

4. Discussion

Influenza virus binds to the special receptors of ciliated columnar epithelial cells on the surface of the respiratory tract to infest the cells after entering the respiratory tract and then replicates. The new virus particles are continuously being released and re-infection spread more to other cells, thus allowing the virus to replicate to higher titers or to establish a continuous infection process (Hutchinson, 2018). As a result, inflammatory factors are greatly amplificated, leading to clinical symptoms such as respiratory distress and coagulation dysfunction (König

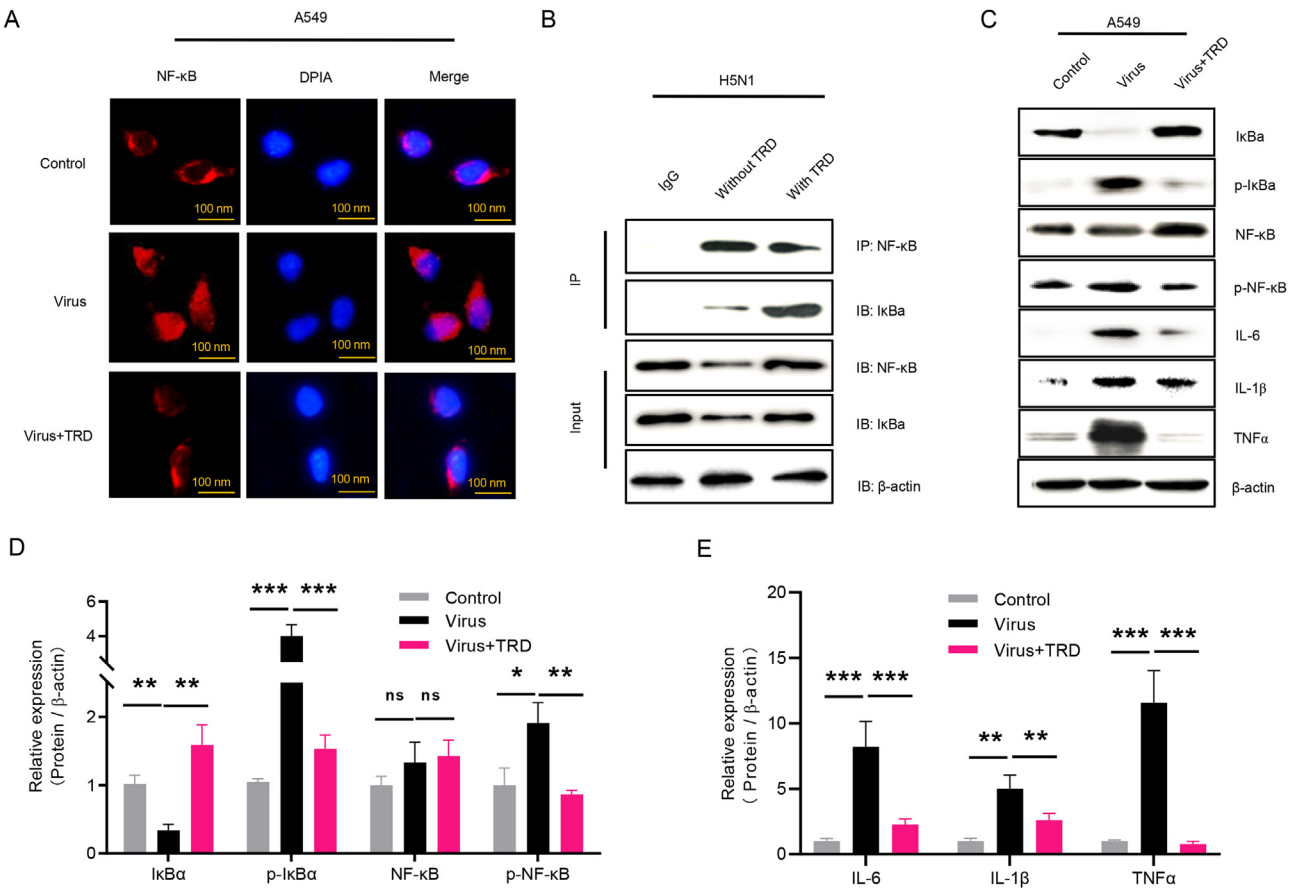

Fig. 4. TRD inhibited the activation of NF-κB signaling pathway. **A** After A549 cells infection with H5N1 at the MOI of 0.1, the cells were treated with solvents DMSO and TRD for 24 h. The nucleus was stained with DAPI, and the NF-κB were detected (scale bar 100 nm). **B** Immunoprecipitation assay verified that TRD treatment inhibited the separation of NF-κB and IκBa after A549 cells were infected with influenza virus. IgG was used as a negative control. **C** The total protein expression level of IκBa, *p*-IκBa and NF-κB, p–NF–κB, as well as TNF-α and IL-6 in lung tissues after infected influenza virus. The whole cell extract was analyzed by Western blotting, using β-actin as a control. **D** Quantification of NF-κB, IκBa and *p*-IκBa expression level in Fig. 4C. **E** Quantification of IL-6, IL-1β and TNFα expression level in Fig. 4C.

et al., 2010). Existing vaccines have limited resistance to mutant strains, and available antiviral drugs had certain side effects. Thus, the re-used of old drugs is also a good strategy, which can accelerate the development of new antiviral drugs against influenza viruses (Haasbach et al., 2017). In this study, we investigated the role of anti-fungal drug TRD in the treatment of infection with H5N1. As expected, we found that it was strongly effective in restricting influenza virus infection and replication without toxicity for cell proliferation.

In addition, TRD treatment effectively protected H5N1 influenza virus-infected mice from death. At a dose of 400 mg/kg/d, the drug did not cause pathological damage *in vivo*, which is consistent with the *in vitro* observations. Conversely, at this dose, TRD attenuated acute lung injury induced by influenza virus infection and improved survival in infected mice (Fig. 2). This suggested that TRD might be a potential drug against influenza virus infection. We will investigate the effect of TRD on other respiratory viruses or other influenza strains in the future.

Remarkably, the early induction of cytokines and chemokines was associated with the formation of human symptoms and disease progression. Previous studies suggested that cytokines (*IFN-α*, *IFN-γ*, and *IL-2*, as well as *TNF-α* and *IL-6*) were related to the morbidity during influenza virus infection (Morales-García et al., 2012; García-Ramírez et al., 2015; Bai et al., 2021). Chemokines (such as *CCL2*, *CCL3*, *CXCL2*, and *CXCL10*) induced innate-immune cells (such as lymphocytes and monocytes) to recruit to the lung tissues, thereby releasing more inflammatory cytokines to intensify the cytokine storm and to further damage the lung tissues (Nanki et al., 2016; Bakogiannis et al., 2019). Importantly, influenza virus infection promotes the recruitment of immune cells to the lung tissues, which constitutes the immune defense mechanism of host resistance viral infections (Cole and Ho, 2017). Excessive cytokines and chemokines lead to a sharp amplification of the inflammatory response, which is also a sign of influenza virus pathogenic effects. The release of a large number of pro-inflammatory cytokines chemoattract more immune cells to construct a positive feedback loop, but they induce cytokine storm when reaching a certain threshold (Gu et al., 2019). This is the main reason for morbidity and mortality caused by influenza virus. Here, we proved the potential role of TRD in anti-virus by regulating this process. In addition, the recruitment of immune cells and abnormalities in the cytokine cascade were able to predict disease severity during influenza virus infection, especially for HPAIV (Teijaro et al., 2011; 2014). Consistently, we found that the expression of cytokines and chemokines were strongly down-regulated after TRD treatment (Fig. 3), and the percentages of neutrophils were significantly reduced after influenza virus infection (Fig. 5). Importantly, our results showed that TRD played important roles in suppressing inflammation responses and related diseases caused by cytokine storm.

The regulation of host immune response has the potential advantage of the inflammatory response caused by virus infection. Its main feature is the activation of multiple signaling pathways (such as NF-κB) by coordinating the expression of pro-inflammatory and anti-inflammatory mediators, thereby regulating the host immune reaction (Sun et al., 2018; Bergmann and Elbahesh, 2019; Li et al., 2020). NF-κB is a protein complex that is responsible for DNA transcription, cytokine production, and cell survival. This complex played critical role in regulating immunity and participating in inflammatory response (Ma et al., 2020).

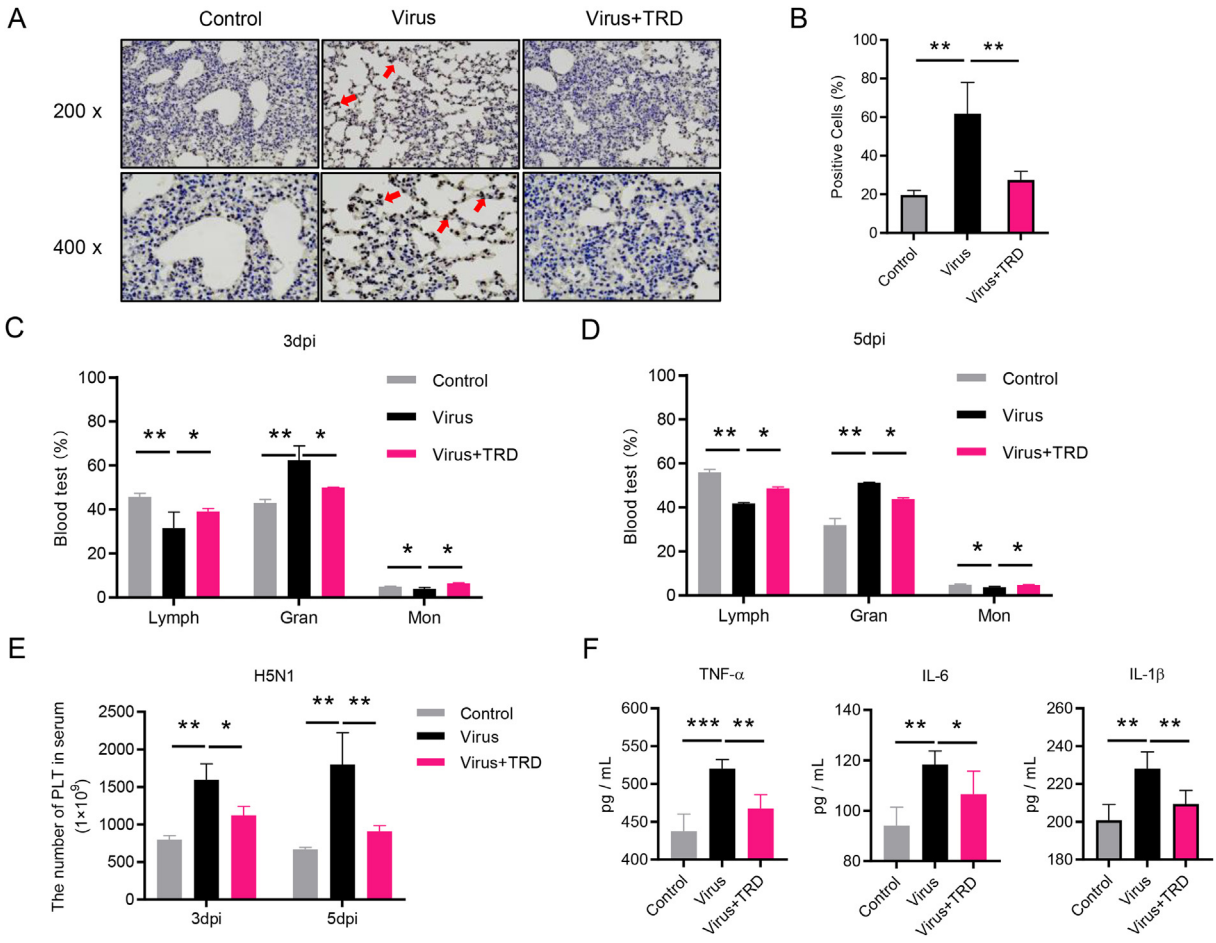

Fig. 5. TRD improved the prognosis of mice after fatal infection with H5N1. **A** Immunohistochemical analysis of p–NF–κB expression intensity in lung tissue after influenza virus infection. The upper panels were the 200-fold observation results, and the lower panels were the 400-fold, red arrows indicated positive cells. **B** Quantification the number of positive cells in p–NF–κB. **C-D** The percentage number of immune cells in mouse serum was determined on the 3dpi (**C**) and 5dpi (**D**) after virus infection by hematological analysis, lymphocytes (Lymph), neutrophils (Gran) and monocyte (Mon). **E** The number of platelets (PLT) in mouse serum was measured on the 3dpi and 5dpi after virus infection by hematological analysis. **F** ELISA assay detected the total protein content of cytokines (TNF-α, IL-6, and IL-1β) in mouse serum.

Moreover, its abnormal expression is related to cancer, inflammation, and auto-immune diseases, septic shock, viral infection, and immune development abnormalities (Di Donato et al., 2012). During the virus attacking, it induces the phosphorylation of the NF-κB essential modulator (NEMO) and activates the IKK complex. As a result, IκBα is phosphorylated, leading to the release of NF-κB heterodimers (P65/P50) and promoting its transfer to the nucleus, thereby regulating the expression of inflammatory cytokines (Liu et al., 2017). When exploring the anti-influenza virus effect of TRD through transcriptome sequencing, we found that the NF-κB signaling pathway was significantly enriched, which indicated that the pathway might be involved in the process. It has been reported that influenza virus infection induces the activation of NF-κB, and promoted the expression of inflammatory factors (such as *TNF-α* and *IL-6*), thereby accelerating the process of inflammation (Wang et al., 2007). Our results revealed that TRD treatment could inhibit the separation of NF-κB and IκBa (Fig. 4) and significantly inhibited NF-κB expression in lung tissues at day 5 post infection (Fig. 5). Therefore, it might be a new drug for reducing the inflammation induced by influenza virus infection.

5. Conclusions

In conclusion, our study found that TRD could suppress influenza infection *in vitro* and *in vivo*, and increase the survival rate of H5N1-infected mice. Further study revealed the unexpected role of TRD in inactivating the influenza-induced cytokine storms and inflammation responses via regulating the NF-κB signaling pathway. Those results suggest TRD is a novel type of antiviral candidate drug against influenza virus.

Data availability

All the data generated during the current study are included in the manuscript.

Ethics statement

Animal experiments were conducted in accordance with the Chinese Laboratory Animal Welfare and Ethics Guidelines (GB 14925-2001). The agreement was approved by the Animal Welfare and Ethics Committee of the Chinese Academy of Agricultural Sciences (license number SCXK-2012-017).

Author contributions

Chaoxiang Lv: investigation, data curation, writing – original draft. Yuanguo Li: investigation, data curation. Tiecheng Wang: investigation, data curation, investigation. Qiqi Zhang: investigation. Jing Qi: investigation. Mingwei Sima: investigation. Entao Li: investigation. Tian Qin: investigation. Zhuangzhuang Shi: investigation. Fangxu Li: investigation. Xuefeng Wang: conceptualization, methodology. Weiyang Sun: investigation. Na Feng: conceptualization. Songtao Yang: conceptualization.

Xianzhu Xia: conceptualization, supervision. Ningyi Jin: conceptualization, methodology, writing - review&editing, supervision. Yifa Zhou: conceptualization, methodology, writing - review&editing, supervision. Yuwei Gao: conceptualization, methodology, writing - review&editing, supervision. All authors reviewed the manuscript.

Conflict of interest

The authors declare that they have no conflict of interest.

Acknowledgements

This work was supported by the Chinese National Natural Science Foundation of China (grant number: 31970502), the National Key Research and Development Program of China (2021YFC2301701, 2020ZX10001-016-003 and ZX10304402-003-006).

Appendix A. Supplementary data

Supplementary data to this article can be found online at https://doi.org/10.1016/j.virs.2022.11.010.

References

Arweiler, N.B., Auschill, T.M., Sculean, A., 2012. Antibacterial effect of taurolidine (2%) on established dental plaque biofilm. Clin. Oral Invest. 16, 499–504.
Bai, Y., Lian, P., Li, J., Zhang, Z., Qiao, J., 2021. The active GLP-1 analogue liraglutide alleviates H9N2 influenza virus-induced acute lung injury in mice. Microb. Pathog. 150, 104645.
Bakogiannis, C., Sachse, M., Stamatelopoulos, K., Stellos, K., 2019. Platelet-derived chemokines in inflammation and atherosclerosis. Cytokine 122, 154157.
Bedrosian, I., Sofia, R.D., Wolff, S.M., Dinarello, C.A., 1991. Taurolidine, an analogue of the amino acid taurine, suppresses interleukin 1 and tumor necrosis factor synthesis in human peripheral blood mononuclear cells. Cytokine 3, 568–575.
Bergmann, S., Elbahesh, H., 2019. Targeting the proviral host kinase, FAK, limits influenza a virus pathogenesis and NFkB-regulated pro-inflammatory responses. Virology 534, 54–63.
Betakova, T., Kostrabova, A., Lachova, V., Turianova, L., 2017. Cytokines induced during influenza virus infection. Curr. Pharmaceut. Des. 23, 2616–2622.
Braumann, C., Gutt, C.N., Scheele, J., Menenakos, C., Willems, W., Mueller, J.M., Jacobi, C.A., 2009. Taurolidine reduces the tumor stimulating cytokine interleukin-1beta in patients with resectable gastrointestinal cancer: a multicentre prospective randomized trial. World J. Surg. Oncol. 7, 32.
Cole, S.L., Ho, L.P., 2017. Contribution of innate immune cells to pathogenesis of severe influenza virus infection. Clin. Sci. (Lond.) 131, 269–283.
Di Donato, J.A., Mercurio, F., Karin, M., 2012. NF-κB and the link between inflammation and cancer. Immunol. Rev. 246, 379–400.
Doddakula, K.K., Neary, P.M., Wang, J.H., Sookhai, S., O'Donnell, A., Aherne, T., Bouchier-Hayes, D.J., Redmond, H.P., 2010. The antiendotoxin agent taurolidine potentially reduces ischemia/reperfusion injury through its metabolite taurine. Surgery 148, 567–572.
García-Ramírez, R.A., Ramírez-Venegas, A., Quintana-Carrillo, R., Camarena, Á.E., Falfán-Valencia, R., Mejía-Aranguré, J.M., 2015. TNF, IL-6, and IL-1β polymorphisms are associated with severe influenza A (H1N1) virus infection in the Mexican population. PLoS One 10, e0144832.
Gu, Y., Hsu, A.C., Pang, Z., Pan, H., Zuo, X., Wang, G., Zheng, J., Wang, F., 2019. Role of the innate cytokine storm induced by the influenza A virus. Viral Immunol. 32, 244–251.
Haasbach, E., Müller, C., Ehrhardt, C., Schreiber, A., Pleschka, S., Ludwig, S., Planz, O., 2017. The MEK-inhibitor CI-1040 displays a broad anti-influenza virus activity in vitro and provides a prolonged treatment window compared to standard of care in vivo. Antivir. Res. 142, 178–184.
Haro, C., 2019. Taurolidina, un antiséptico para la prevención de infeccionesasociadas a catétervenoso central [Taurolidine, an antiseptic for the prevention of central venous catheter-related infections]. Rev. ChilenaInfectol 36, 414–420.
Hutchinson, E.C., 2018. Influenza virus. Trends Microbiol. 26, 809–810.
Jacobi, C.A., Menenakos, C., Braumann, C., 2005. Taurolidine-a new drug with anti-tumor and anti-angiogenic effects. Anti Cancer Drugs 16, 917–921.
Kain, T., Fowler, R., 2019. Preparing intensive care for the next pandemic influenza. Crit. Care 23, 337.
König, R., Stertz, S., Zhou, Y., Inoue, A., Hoffmann, H.H., Bhattacharyya, S., Alamares, J.G., Tscherne, D.M., Ortigoza, M.B., Liang, Y., Gao, Q., Andrews, S.E., Bandyopadhyay, S., Jesus, P., Tu, B.P., Pache, L., Shih, C., Orth, A., Bonamy, G., Miraglia, L., Ideker, T., García-Sastre, A., Young, J.A., Palese, P., Shaw, M.L., Chanda, S.K., 2010. Human host factors required for influenza virus replication. Nature 463, 813–817.
Lawrence, T., 2009. The nuclear factor NF-kappaB pathway in inflammation. Cold Spring Harbor Perspect. Biol. 1, a001651.
Lee, H.K., Tang, J.W., 2015. Extended full-genome phylogenetic analysis of the first human A/H5N1 avian influenza case in North America. Infect. Genet. Evol. 32, 327–329.
Lewis, N.S., Banyard, A.C., Whittard, E., Karibayev, T., Kafagi, T., Chvala, I., Byrne, A., Akberovna, S., King, J., Harder, T., Grund, C., Essen, S., Reid, S.M., Brouwer, A., Zinyakov, N.G., Tegzhanov, A., Irza, V., Pohlmann, A., Beer, M., Fouchier, R.A.M., Akievich, S., Brown, I.H., 2021. Emergence and spread of novel H5N8, H5N5 and H5N1 clade 2.3.4.4 highly pathogenic avian influenza in 2020. Emerg. Microb. Infect. 10, 148–151.
Li, J., Jie, X., Liang, X., Chen, Z., Xie, P., Pan, X., Zhou, B., Li, J., 2020. Sinensetin suppresses influenza a virus-triggered inflammation through inhibition of NF-κB and MAPKs signalings. BMC Complement Med. Ther. 20, 135.
Liu, T., Zhang, L., Joo, D., Sun, S.C., 2017. NF-κB signaling in inflammation. Signal Transduct. Targeted Ther. 2, 17023.
Ma, Q., Huang, W., Zhao, J., Yang, Z., 2020. Liu Shen Wan inhibits influenza a virus and excessive virus-induced inflammatory response via suppression of TLR4/NF-κB signaling pathway in vitro and in vivo. J. Ethnopharmacol. 252, 112584.
Mehrbod, P., Abdalla, M.A., Fotouhi, F., Heidarzadeh, M., Aro, A.O., Eloff, J.N., McGaw, L.J., Fasina, F.O., 2018. Immunomodulatory properties of quercetin-3-O-α-L-rhamnopyranoside from Rapanea melanophloeos against influenza a virus. BMC Compl. Alternative Med. 18, 184.
Morales-García, G., Falfán-Valencia, R., García-Ramírez, R.A., Camarena, Á., Ramirez-Venegas, A., Castillejos-López, M., Pérez-Rodríguez, M., González-Bonilla, C., Grajales-Muñíz, C., Borja-Aburto, V., Mejía-Aranguré, J.M., 2012. Pandemic influenza A/H1N1 virus infection and TNF, LTA, IL1B, IL-6, IL8, and CCL polymorphisms in Mexican population: a case-control study. BMC Infect. Dis. 12, 299.
Mulero, M.C., Huxford, T., Ghosh, G., 2019. NF-κB, IκB, and IKK: integral components of immune system signaling. Adv. Exp. Med. Biol. 1172, 207–226.
Nanki, T., 2016. [Treatment for rheumatoid arthritis by chemokine blockade]. Nihon RinshoMeneki Gakkai Kaishi 39, 172–180.
Neary, P.M., Hallihan, P., Wang, J.H., Pfirrmann, R.W., Bouchier-Hayes, D.J., Redmond, H.P., 2014. The evolving role of taurolidine in cancer therapy. Ann. Surg Oncol. 17, 1135–1143.
Pleschka, S., 2013. Overview of influenza viruses. Curr. Top. Microbiol. Immunol. 370, 1–20.
Sun, H., Yao, W., Wang, K., Qian, Y., Chen, H., Jung, Y.S., 2018. Inhibition of neddylation pathway represses influenza virus replication and pro-inflammatory responses. Virology 514, 230–239.
Sutton, T.C., 2018. The pandemic threat of emerging H5 and H7 avian influenza viruses. Viruses 10, 461.
Taubenberger, J.K., Kash, J.C., 2010. Influenza virus evolution, host adaptation, and pandemic formation. Cell Host Microbe 7, 440–451.
Teijaro, J.R., Walsh, K.B., Cahalan, S., Fremgen, D.M., Roberts, E., Scott, F., Martinborough, E., Peach, R., Oldstone, M.B., Rosen, H., 2011. Endothelial cells are central orchestrators of cytokine amplification during influenza virus infection. Cell 146, 980–991.
Teijaro, J.R., Walsh, K.B., Rice, S., Rosen, H., Oldstone, M.B., 2014. Mapping the innate signaling cascade essential for cytokine storm during influenza virus infection. Proc. Natl. Acad. Sci. U. S. A. 111, 3799–3804.
Tian, H., Zhou, S., Dong, L., Boeckel, T.P., Cui, Y., Newman, S.H., Takekawa, J.Y., Prosser, D.J., Xiao, X., Wu, Y., Cazelles, B., Huang, S., Yang, R., Grenfell, B.T., Xu, B., 2015. Avian influenza H5N1 viral and bird migration networks in Asia. Proc. Natl. Acad. Sci. U. S. A. 112, 172–177.
Viboud, C., Simonsen, L., Fuentes, R., Flores, J., Miller, M.A., Chowell, G., 2016. Global mortality impact of the 1957-1959 influenza pandemic. J. Infect. Dis. 213, 738–745.
Wang, W., Ye, L., Ye, L., Li, B., Gao, B., Zeng, Y., Kong, L., Fang, X., Zheng, H., Wu, Z., She, Y., 2007. Up-regulation of IL-6 and TNF-alpha induced by SARS-coronavirus spike protein in murine macrophages via NF-kappaB pathway. Virus Res. 128, 1–8.
Xue, Q., Liu, H., Zhu, Z., Yang, F., Ma, L., Cai, X., Xue, Q., Zheng, H., 2018. Seneca Valley Virus 3Cpro abrogates the IRF3- and IRF7-mediated innate immune response by degrading IRF3 and IRF7. Virology 518, 1–7.